Quantum Mechanical and Spectral Comparative Study of 1-p-Nitro-Benzoyl-Benzo[f]Quinolinium Methylid and 1-p-Nitrobenzoyl-2,3-Dicarbomethoxy-Pyrrolo-[1,2a]-Benzo[f]Quinoline

ANTONINA GRITCO TODIRASCU, CEZARINA MOROSANU, DOINA PARTENIE, DANA ORTANSA DOROHOI*, DORINA CREANGA[1]
Alexandru Ioan Cuza University, Faculty of Physics, 11 Blvd. Carol I, 700506, Iasi, Romania

The quantum mechanical and spectral study of two related compounds, namely, 1-p-nitro-benzoyl-benzo[f]quinolinium methylid (BF1) and its cycloadduction derivative 1-p-nitro-benzoyl-2,3-dicarbomethoxy-pyrrolo-[1,2a]-benzo[f]quinoline (BF2) was carried out. Some electro-optical parameters in ground state were estimated by ab initio method. The solvatochromic behavior of the visible spectrum absorption band of the studied molecules in solvents with different macroscopic electro-optical proprieties was analyzed in order to estimate some microscopic molecular parameters of BF1 and BF2 in the excited state. Thus it was evidenced that, by excitation, the increase of BF1dipole moment and electric polarizability occurred while for BF2 either the increase or the decrease of these two parameters was found. The study is of practical importance for further synthesis of new derived compounds with potential applications in life sciences.

Keywords: structural modeling, excited state dipole moment, excited state polarizability.

The cycloaddition reactions of cycloimmonium ylids were studied by various research teams, the term ylid being introduced by G. Wittig and Felletschin [1]. In [2] the cycloadducts derived from cycloimmonium ylids and triphenylcyclopropene were presented. In [3-6] consecutive dipolar cycloadditions of cycloimmonium ylids to benzyne were studied. The 3-2 dipolar cycloaddition of cycloimmonium ylids to dienophiles was applied in a two step preparation method of steroid analogous with anticipated biological activity [7], including antiviral [8] and anticancer [9], antimicrobial, antifungal, anti-androgenic effects etc. The stable cycloimmonium ylids that provide various cycloadducts have also interesting applications such as analytical reagents [10], semi-conducting materials [11], or substances with anti-microbial and antifungal action. They are used in various heterocycle syntheses of new classes of aza-heterocycle compounds and as acid-basic indicators, by their specific color changing. In the present paper we studied one benzo[f]quinolinium ylid (denoted as BF1) and one cycloadduct of this ylid (denoted as BF2), having the same side substituents, to evidence solvatochromic behavior and to estimate some microscopic molecular parameters. The structural and energetic parameters provided by quantum mechanical modeling for the two related structures as well as their spectral behavior in diluted solution are presented comparatively in this paper.

Experimental part

Materials and methods

The synthesis of BF1 cycloimmonium ylid and of BF2 cycloadduct was carried out according to Zugravescu & Petrovanu [6]. The synthesis reaction of BF2 is presented in figure 1. Benzo[f]quinoline-p-nitro-phenacylide, (fig. 1 left) leads to 1-p-nitrobenzoyl-2,3-dicarbomethoxy-pyrrolo-(1,2-a)-benzo[f]quinoline, i.e. BF2 (fig. 1 right) in the presence of methyl-acetylene-dicarboxylate, after a dehydrogenation process [6].

Spectral investigation was carried out using SHIMADZU spectrophotometer PharmaSpec 1700 with 1 cm quartz cells. The device is supplied with deuterium lamp and respectively halogen tungsten lamp for visible domain and for UV radiation spectrum; the accuracy of wavelength recording was of 0.5 nm.

The electronic absorption spectra (EAS) from visible range were recorded in 10^4 diluted solutions, in various solvents with different polarities (table 1).

The solvents and all reagents were high purity ones as checked by infrared spectra. 95.0-98.0% sulfuric acid (ACS reagent, from Sigma Aldrich) was used to test the solutions spectral response to protonation.

Solvatochromic study was developed by applying basic theories, that provided correlations between EAS wavenumbers and solvent macroscopic parameters like

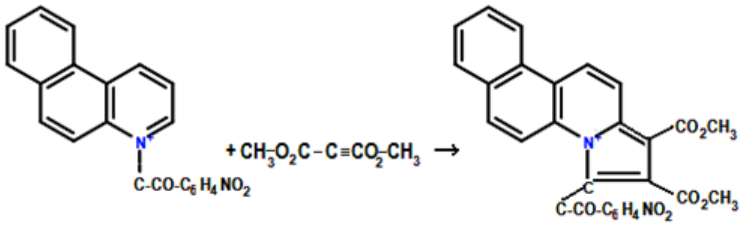

Fig. 1. Synthesis reaction of 1-p-nitrobenzoyl-2,3-dicarbomethoxy-pyrrolo-[1,2- a]-benzo[f]quinoline from benzo[f]quinolinium methylid in p-nitro-benzoyl and methyl-acetylene-dicarboxylate

* *email: mdor@uiac.ro; Phone: 0749641954*

	Solvent	Refractive index, *n*	Dielectric constant, *ε*
1	*o*-Xylene	1.505	2.28
2	*n*-Butyl acetate	1.395	5.10
3	1, 2 Dichloroethane	1.4448	10.10
4	Benzyl alcohol	1.539	13.30
5	Acetonitrile	1.357	36.00

Table 1
SOLVENT MACROSCOPIC PARAMETERS

refractive index (n) and dielectric constant (e) [12-16]. HyperChem molecular modeling program (quantum mechanics method PM3), was applied, based on Polak-Ribiere optimization algorithm, restricted Hartree-Fock wavefunction, the convergence limit of 0.0001 kcal/mol and RMS gradient of 0.0001 kcal/(Å mol).

Results and discussions

The optimized structures of studied BF1 and BF2 compounds having the same three side substituents ($COCH_3$, $COCH_3$ and $COC_6H_4NO_2$), are given in figure 2, where total charge density maps can be seen as well as the dipole moment orientations in the ground state of isolated molecules.

Remarkable high charge density in BF1 (fig. 2a) around side substituent $COC_6H_4NO_2$ could explain the sensitivity to proton attack in acidic solution as shown experimentally further bellow.

Comparing BF1 with BF2 (fig. 2 b), the quantum-chemical modeling revealed that the charge density of the largest substituent ($COC_6H_4NO_2$) was redistributed in BF2 toward the heterocycle, while the charges corresponding to the carbanion (C_{24}) and to the heterocycle nitrogen (N_1) were diminished with about the same amount: 0.356 and respectively 0.343 *e* (*e*- electron electric charge) (table 2).

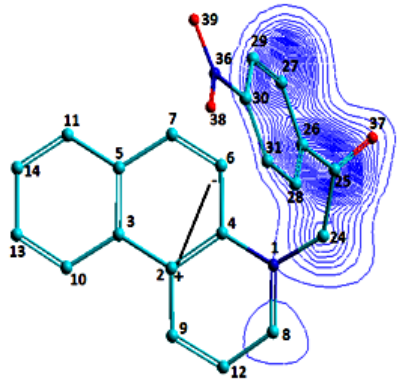

Fig. 2 a. Charge density and dipole moment - μ_g for BF1 optimized structure

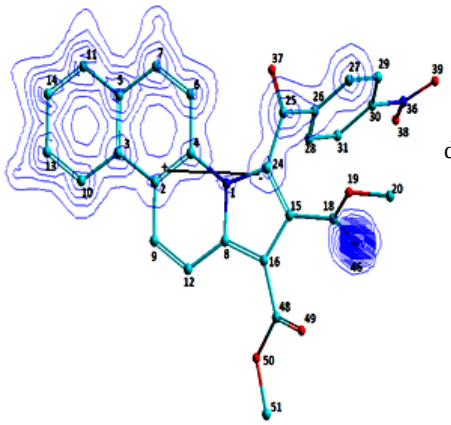

Fig. 2 b. Charge density and dipole moment- μ_g for optimized structure for BF2

Atomic charges on BF1				Atomic charges on BF2			
Atom	Charge	Atom	Charge	Atom	Charge	Atom	Charge
N_1	0.927	C_{14}	-0.081	N_1	0.571	C_{20}	0.072
C_2	0.094	C_{24}	-0.716	C_2	-0.006	C_{24}	-0.373
C_3	-0.049	C_{25}	0.416	C_3	-0.021	C_{25}	0.424
C_4	-0.332	C_{26}	-0.091	C_4	-0.155	C_{26}	-0.105
C_5	-0.011	C_{27}	-0.083	C_5	-0.035	C_{27}	-0.072
C_6	-0.073	C_{28}	-0.094	C_6	-0.139	C_{28}	-0.076
C_7	-0.097	C_{29}	-0.016	C_7	-0.054	C_{29}	-0.019
C_8	-0.480	C_{30}	-0.397	C_8	-0.172	C_{30}	-0.383
C_9	-0.220	C_{31}	-0.016	C_9	-0.110	C_{31}	-0.011
C_{10}	-0.083	N_{36}	1.305	C_{10}	-0.097	N_{36}	1.304

Table 2
ELECTRIC CHARGE DISTRIBUTION FOR THE OPTIMIZED MOLECULES

C_{11}	0.095	O_{37}	-0.312	C_{11}	-0.084	O_{37}	-0.304
C_{12}	0.029	O_{38}	-0.598	C_{12}	-0.041	O_{38}	-0.595
C_{13}	-0.099	O_{39}	-0.598	C_{13}	-0.087	O_{39}	-0.595
				C_{14}	-0.091	O_{46}	-0.363
				C_{15}	-0.038	C_{48}	0.456
				C_{16}	-0.161	O_{49}	-0.372
				C_{18}	0.441	O_{50}	-0.267
				O_{19}	-0.253	C_{51}	0.074

Table 2
Continuated

The charges on the atoms of carbonyl group (C_{25}, O_{37}) bound to carbanion remained approximately the same and also the charge of the nitrogen (N_{36}) from the nitro group of the main substituent. But the energetic parameters of molecule ground state (table 3) appeared to be enhanced with over 40% following chemical transformation of BF1 ylid into BF2 cycloadduct. Transition energy *DE* was also increased with about 10%.

Electro-optical microscopic parameters - polarizability and electric dipole moment (table 3) increased with about 30 and 40% respectively. The electronic transition with intramolecular charge transfer occurs, as known [17-18] along the ylid bond, i.e. almost orthogonally on the direction of dipole moment in the ground state, μ_g, so that the interaction between ylid and solvent in the excited state is practically vanishing.

Ylid carbanion, with largest substituent bearing considerable electric charge (fig. 2a), could be rather easily oriented around the dipole moment axis in the solvent reactive field.

Since in the BF2 cycloadduct the dipole moment is lying almost parallel to the same large side substituent while the former BF1 ylid bond was stabilized spatially by the carbons provided through the addition reaction (fig. 2b), the relative movement of BF2 parts - separated formally by the dipole moment axis, became less probable - even the cycloadduct has a higher value of the dipole moment (table 3).

The molecular energetic parameters in the ground state (table 2) appeared to be enhanced with over 40% following chemical transformation of ylid into cycloadduct; transition energy *DE* between Highest Occupied Molecular Orbital (HOMO) and Lowest Unoccupied Molecular Orbital (LUMO) has also increased with about 10%.

Electro-optical microscopic parameters – polarizability and electric dipole moment in the ground state (table 3) increased with about 30% and 40% respectively.

According to figure 3, spatial distribution of molecular orbitals in BF1 is strongly changed from HOMO (fig. 3 a) to LUMO (fig. 3 b), by expanding toward the $COC_6H_4NO_2$ side substituent following light absorption; experimental study of solvent effect emphasized also the changing of dipole moment and electric polarizability in the excited state. In the case of BF2 the presence of addition cycle atoms, (fig. 4), has restricted the mobility of molecular electron clouds, so that the differences between HOMO and LUMO seem to be rather difficult to observe - with no shift toward the $COC_6H_4NO_2$ side substituent.

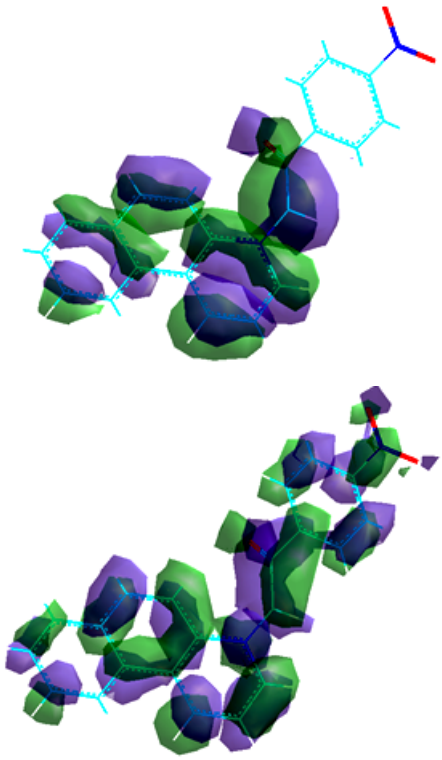

Fig. 3. Frontier orbitals of BF1: a) left- Highest Occupied Molecular Orbital (HOMO); b) right-Lowest Unoccupied Molecular Orbital (LUMO)

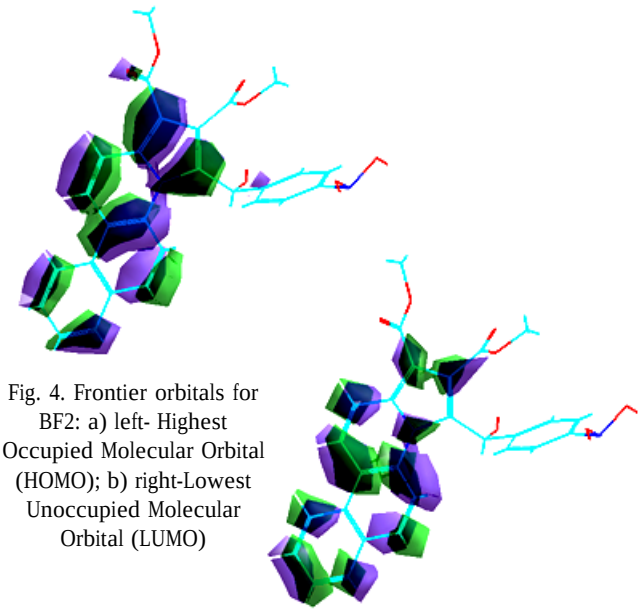

Fig. 4. Frontier orbitals for BF2: a) left- Highest Occupied Molecular Orbital (HOMO); b) right-Lowest Unoccupied Molecular Orbital (LUMO)

Energetic parameters	Ylid (BF1) in isolated state	Energetic parameters	Cycloadduct (BF2) in isolated state
Total energy (kcal/mol)	-90026.901	Total energy (kcal/mol)	-134947.66
Binding energy (kcal/mol)	-4652.634	Binding energy (kcal/mol)	-6286.97
Heat of formation (kcal/mol)	70.1607	Heat of formation (kcal/mol)	-92.1954
E_{HOMO} (eV)	-8.175156	E_{HOMO} (eV)	-8.939749
E_{LUMO} (eV)	-1.345432	E_{LUMO} (eV)	-1.52361
ΔE (ev)	-6.829724	ΔE (ev)	-7.416139
Molecular descriptor	Ylid (BF1) in isolated state	Molecular descriptor	Cycloadduct (BF2) in isolated state
Surface aria (A^2)	543.99	Surface aria (A^2)	696.24
Volume (A^3)	927.12	Volume (A^3)	1230.50
Polarizability (A^3)	37.70	Polarizability (A^3)	49.06
Dipole moment (D)	5.83	Dipole moment (D)	8.27

Table 3
RESULTS OF COMPUTATIONAL STUDY BASED ON QUANTUM CHEMICAL APPROACH

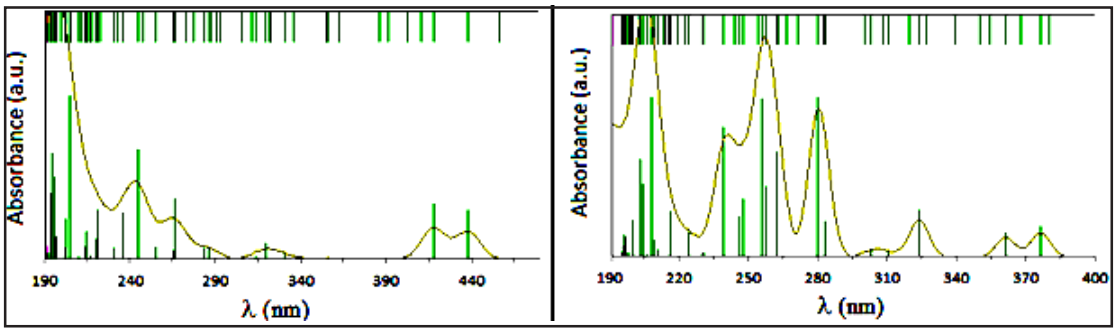

Fig. 5. Simulated electronic spectra of isolated molecules (gas) presented by main absorption transitions (vertical lines) and their approximate envelope; a, left) ylid (BF1); b, right) cycloadduct (BF2)

In figure 5 a, b the simulated electronic absorption transitions are presented for the two compounds.

Since the experimental study was focused on the spectral behaviour of EAS in the visible range, the discussion of both simulated and recorded spectra will be carried out with details for these transitions.

In the simulated spectra the two electronic transitions of BF2 at largest wavelengths (fig. 5 b) are shifted toward the blue domain with about 500 nm compared to BF1 (fig. 5 a).

The visible electronic absorption band of BF1 has been assigned to a transition with intramolecular charge transfer from the carbanion non-participant electronic level toward the heterocycle anti-bonding π orbital (as in the case of some related pyridinium compounds discussed in [19]**). This band has a relatively low intensity, it shifts hypsochromically when passing from nonpolar to polar solvents as well as from non-protic to protic ones, and disappears in acid solutions in which the non-participant electrons of the carbanion are blocked by the free protons (fig. 6). This is concordant with above noticed high charge electron density on the side substituent $COC_6H_4NO_2$, able to attire free protons.

The increase of the conjugation in the case of carbanion disubstituted planar cycloimmonium ylids, determined by electron withdrawing groups attached to the carbanion, caused inhere the shifts of UV absorption bands maximum hypsochromically.

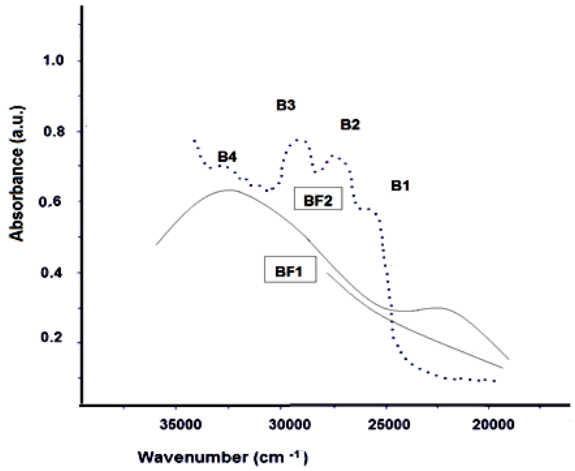

Fig. 6. UV-Vis recorded spectra of BF2 (dashed line with four peaks, B1–B4) and BF1 in n-butyl acetate and n-butyl acetate + propionic acid (beyond)

BF2 bands in the visible range (fig. 6, dashed line) can be assigned to π - π* transitions that do not change to protonation and present smaller shifts to the change of solvent polarity, since the addition cycle of such compounds isolates the substituents from the point of view of π conjugation with heterocycle. The differences between the mathematically modeled spectra (fig. 5) and the spectra recorded in real conditions (fig. 6) could be due also to the simplifying hypotheses of the algorithms underlying the

modeling software. Spectral investigation provided the positions of EAS maxima, i.e. the values of the corresponding wavenumbers recorded in diluted solutions.

The double linear regressions approaching wavenumber dependence on refractive index and dielectric constant corresponding to BF1 band in the visible range as well as to the four vibronic maxima of and BF2 electronic band are (eq. 1-5):

$$\nu_{calc} = 1707.9\, f(\nu) + 8643.8\, f(n) + 15357.8 \quad (1)$$
$$\nu_{calc\,1} = -504.568\, f(\nu) - 4071.8\, f(n) + 25595.3 \quad (2)$$
$$\nu_{calc\,2} = 340.177\, f(\nu) - 1375.77\, f(n) + 27580.9 \quad (3)$$
$$\nu_{calc\,3} = 123.7928\, f(\nu) - 1545.2\, f(n) + 28807.6 \quad (4)$$
$$\nu_{calc\,4} = 146.9179\, f(\varepsilon) - 2313.24\, f(n) + 33492.7 \quad (5)$$

The numerical coefficients of regression equations provided data for calculation of excited state molecular parameters. Last term corresponds to the wavenumber of the studied molecule in isolated state [20-21].

The numerical processing was based on the solvatochromic theory of Bakhshiev [12], where the spectral shift to the passing from isolated state to diluted solution is assigned to universal or volume intermolecular interactions, being described by the next relationships (eq. 6-19):

$$\Delta\nu = \Delta\nu_{cr} + \Delta\nu_{ind} + \Delta\nu_{pol} + \Delta\nu_{disp} \quad (6)$$

$$\Delta\nu = C_1 \cdot f(\varepsilon) + C_2 \cdot f(n) \quad (7)$$

$$C_1 = \frac{2\mu_g(\mu_g - \mu_e \cos\varphi)}{hca^3} + 3KT\frac{\alpha_g - \alpha_e}{hca^3} \quad (8)$$

$$C_2 = \frac{\mu_g^2 - \mu_e^2}{hca^3} - \frac{2\mu_g(\mu_g - \mu_e \cos\varphi)}{hca^3} - 3KT\frac{\alpha_g - \alpha_e}{a^3} + \frac{3}{2}\frac{\alpha_g - \alpha_e}{a^3}\cdot\frac{I_u \cdot I_v}{I_u + I_v} \quad (9)$$

$$f(\varepsilon) = \frac{\varepsilon + 1}{\varepsilon + 2}; \quad f(n) = \frac{n^2 - 1}{n^2 + 2} \quad (10)$$

where Δn is the spectral shift while *C1* and *C2* are coefficients depending on solute and solvent molecules electro-optical parameters, corresponding to orientation-induction and respectively polarization-dispersion interactions; *h* is Planck constant, *K* is Boltzmann constant, *c* is light velocity in free space, *e* and m_e are the electron charge and respectively electron mass; solute radius is *a*, *f* is its oscillator strength, *I* and *I'* are the ionizing potentials of solute and solvent (estimated as-HOMO energy from quantum mechanical modeling of ground state) and j is the angle between μ_g and μ_e.

The term ν_0 from the spectral shift ($\Delta\nu = \nu - \nu_0$) corresponds to the EAS band wavenumber in the isolated (vapour) state. In figure 7 the comparison of experimental data and the result of computational approach can be seen.

Thus, both major types of solute-solvent interactions were taken into account. The contribution of additional, specific interactions, is supposed to be the cause of graphical points spreading in the neighborhood of the theoretical regression lines, as those are not considered in the frame of solvatochromic theory; consequently some

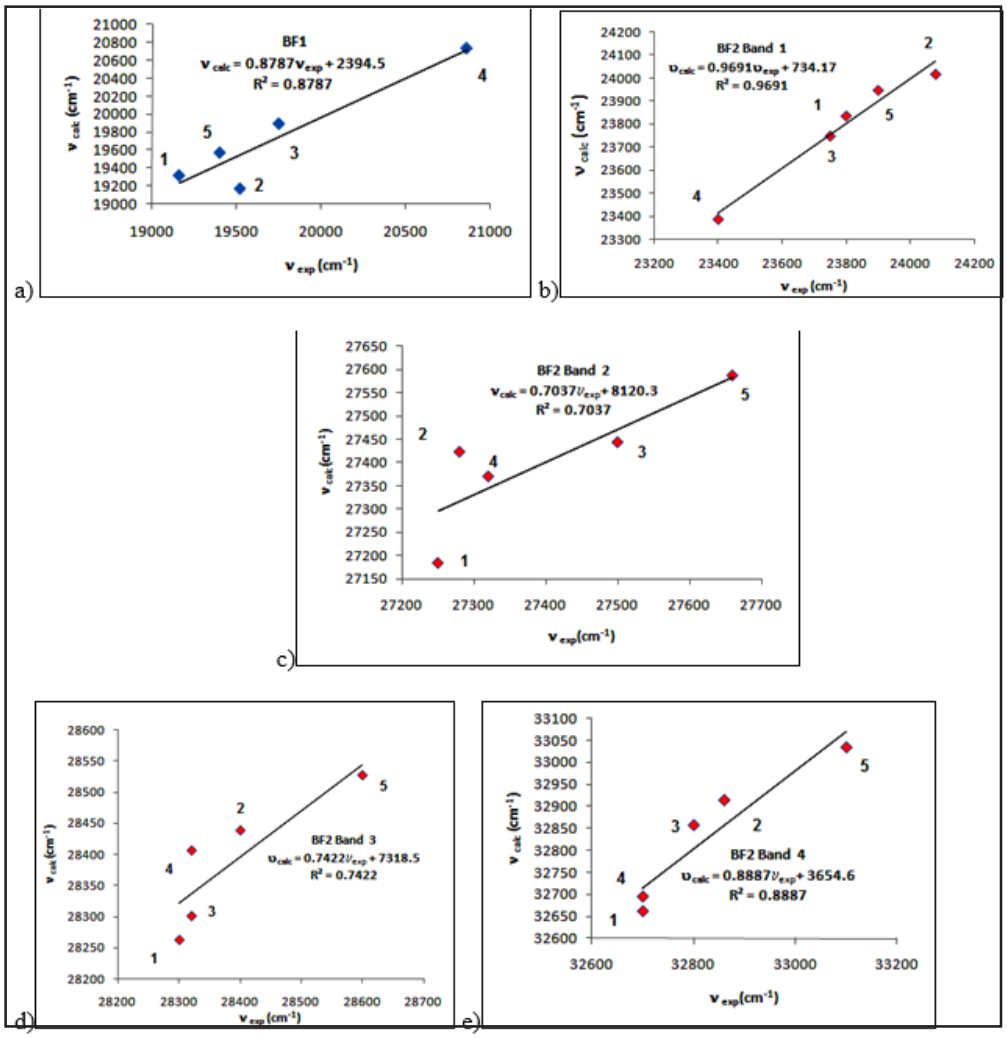

Fig. 7. Comparison of calculated and experimentally recorded wavenumbers in the studied electronic absorption bands of BF1 and BF2 from visible range: a) BF1; b) BF2 band B1; c) BF2 band B2; d) BF2 band B3; e) BF2 band B4

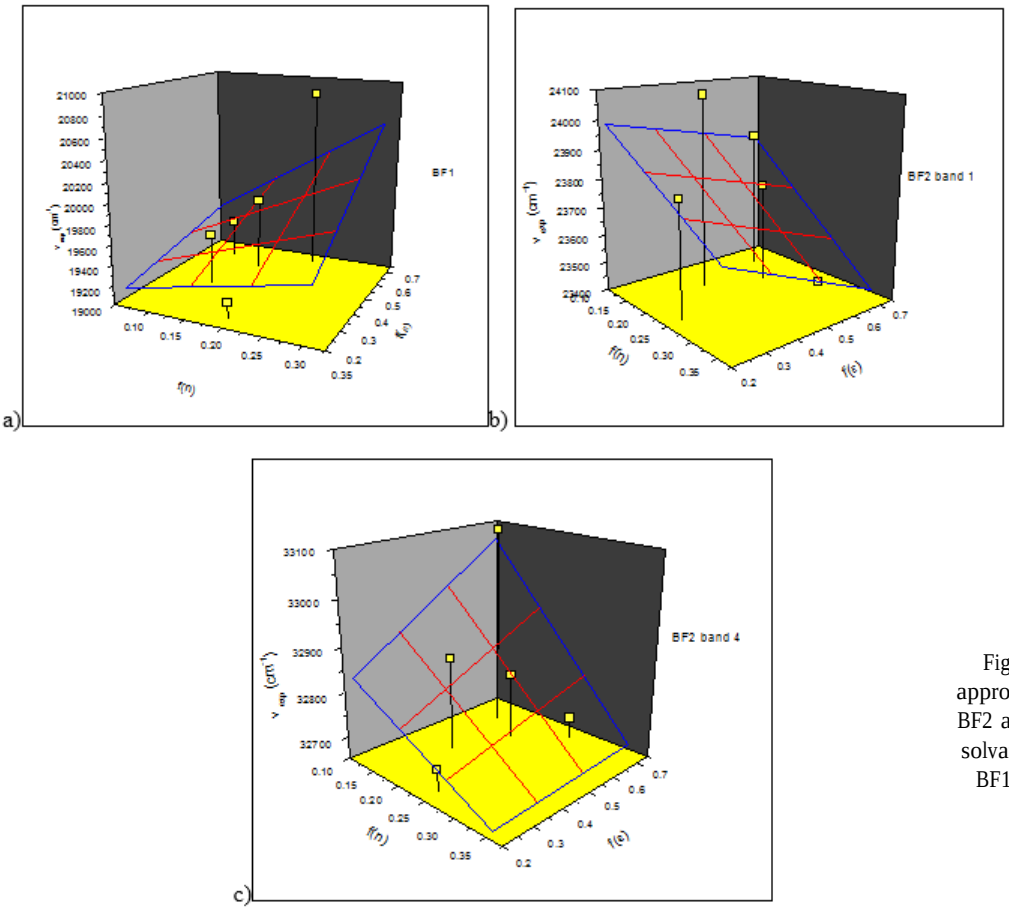

Fig. 8. Regression planes for the approaching solvent effect on BF1 and BF2 according to universal interaction solvatochromic theory: a) the case of BF1; b) BF2 band 1; c) BF2 band 4

correlation coefficients of the regression lines are smaller than 0.9.

In figure 8 the regression planes corresponding to regression relationships given bellow are represented for BF1 and two vibronic bands of BF2 where the highest correlation coefficients were obtained.

To estimate microscopic molecular parameters for BF1 and BF2, the next two equations were used (derived from eqs. 8-9):

$$C1 + C2 = \frac{\mu_g^2}{hca^3} - \frac{\mu_e^2}{hca^3} + \frac{3}{2}\frac{I_u I_v}{I_u + I_v}\frac{\alpha_g}{a^3} - \frac{3}{2}\frac{I_u I_v}{I_u + I_v}\frac{\alpha_e}{a^3} \quad (11)$$

$$C1 = \frac{2\mu_g^2}{hca^3} - \frac{2\mu_g \mu_e \cos\varphi}{hca^3} + \frac{3kT\alpha_g}{a^3} - \frac{3kT\alpha_e}{a^3} \quad (12)$$

First, the excited state polarizability α_e, could be written as a function of the excited state dipole moment μ_e^2, then, a second order equation in μ_e was obtained having cos φ as parameter. This equation discriminant should be positive in order to get real numbers as mathematical solutions.

We have found: cosφ ≥ 0.095268 (BF1); cosφ_1 ≥ 0.162543 (BF2 band 1); cos φ_2 ≥ 0.148343 (BF2 band 2); cos φ_3 ≥ 0.152104 (BF2 band 3); cos φ_4 ≥ 0.151706 (BF2 band 4).

It could be seen that the angle between dipole moment in the ground and excited state is higher for the ylid (BF1) than for the cycloadduct (BF2) (cos j being smaller) but for both molecules, the electric vector could be rotated up to about 80 degrees following light absorption.

Replacing in the above equations the appropriate values of cos φ, the μ_e, the dipole moment values with physical meaning were obtained (exemplifying for cos φ =1, i.e. φ=0); further the molecule polarizability in the excited state was calculated (table 4).

Subsequently in the case of BF1 (table 4) the dipole moment diminished about twice (from 5.83 D to 2.20 D) while the electric polarizability has decreased about three times (from 37.7 to 13.25Å^3); in the case of BF2 several percentage diminution of dipole moment were noticed together with over 20% increase of electric polarizability (as in the case of other heterocyle compounds studied in [22]).

In the case of BF2, the excited state dipole moment estimated from experimental data corresponding to band 1 appeared to be higher than in the ground state which

Table 4

MICROSCOPIC PARAMETERS OF STUDIED MOLECULES CALCULATED FOR THE EXCITED STATE

BF1			BF2					
					band 1	band 2	band 3	band 4
μ_g =5.83 D	μ_e (D)	2.20	μ_g =8.27 D	μ_e (D)	9.11	7.58	7.97	7.93
α_g =37.7 Å^3	α_e (Å^3)	13.25	α_g=49.06 Å^3	α_e (Å^3)	58.00	60.54	59.94	60.00

could be related to the putative high influence of the vibration motions.

Conclusions

Changes in the electronic orbitals of benzo[f]quinolinium ylids that occurred through cycloaddition reactions were noticed by the modification of electronic absorption spectra and their sensitivity to solvent action in diluted solutions. The nature of the electronic band from the visible range changed from n-π^* to π-π^* while the influence of the vibrational energies become evident in the vibronic structure of visible range band. Both important types of universal solute-solvent interactions were evidenced in the solvatochromic behavior of studied molecules.

Double linear regression approach according to theoretical formula has allowed calculating wavenumbers, which were close to experimental ones. Some exceptions related to solvents containing carbonyl group suggested specific local interactions at the level of BF2 addition cycle. Further study will be focused on alternative theoretical interpretation based on solvent empirical parameters to take into account the hydrogen bond interactions between solute molecules and solvent ones.

References

1. DO NHAT VAN, RUCINSCHI, E., DRUTA, I., ZUGRAVESCU, I., Bul. Inst. Polit., Iasi, **XXIII** (XXVII) 1977, p. 51.
2. DO NHAT VAN, Thesis, Alexandru Ioan Cuza University, Faculty of Chemistry, 1979.
3. ZUGRAVESCU, I., PETROVANU, M., N-ylid chemistry, Academic Press, N.Y., 1978.
4. RUCINSCHI, E., DO NHAT VAN, DRUTA, I., ZUGRAVESCU, I., Bul. Inst. Polit., **XXIV** (XXVIII), 1978, p. 107.
5. PAWDA, A., 1, 3-Dipolar Cycloaddition Chemistry, Wiley Interscience, NY, 1984.
6. PETROVANU, M., ZUGRAVESCU, I., Cycloaddition Reactions, Academic Press, New York, 1987.
7. BEJAN, V., MOLDOVEANU, C., MANGALAGIU, I. I., Ultrason. Sonochem., **16**, 2009, p. 16312.
8. SAXENA, H., FARIDI, V., Steroids, **72**, 2007, p. 892.
9. WU, J. BATIST G., ZAMIR, L., Anti-Cancer Drug Design, **16**, 2001, p.129.
10. PAWDA, A., 1,3-Dipolar Cycloaddition Chemistry, Wiley Interscience, NY, 1984.
11. LEONTIE, L., OLARIU I., RUSU, G.I., Mater. Chem. Phys., **80**, 2003, p.506.
12. BAKHSHIEV, N.G., Spectroscopy of intermolecular interactions [in Russian], Ed. Nauka, Leningrad, 1972.
13. NADEJDE, C., URSU, L., CREANGA, D., DOROHOI, D., Rev. Chim. (Bucharest), **66**, no. 3, 2015, p.360.
14. DULCESCU, M., STAN C., DOROHOI, D.O., Rev. Chim. (Bucharest), **61**, no. 12, 2010, p. 1219.
15. RESKE, A.M.W., WYSOCKI, S., GRZEGORZ, W.B., Spectrochim. Acta Part A, **62**, 2005, p.1172.
16. HOMOCIANU, M., AIRINEI, A., DOROHOI, D.O., J. Adv. Res. Phys., **2**, 2011, 011105.
17. DOROHOI, D.O., PARTENIE, H., J. Molec. Struct. **293**, 1993, p. 129.
18. DOROHOI, D.O., PARTENIE, D.H., CHIRAN, L.M., ANTON, C., J. Chim. Phys. Phys. Chim. Biol., **91**, 1994, p. 419.
19. CARAC, A., BOSCENCU, R., DEDIU, A.V., BUNGAU, S.G., DINICA, R.M., Rev. Chim. (Bucharest), **68**, no. 7, 2017, p. 1422.
20. HILLARD, L., FOULK, D.S., GOLD, H.S., Anal. Chim. Acta, **133** (3), 1981, p. 319.
21. SIDIR, I., TASAL, E., GULSEVEN, Y., GUNGOR, T., BERBER, H., OGRETIR, C., Int. J. Hydrogen Energy, **34**, 2009, p. 5267.
22. CIUBARA, A.M., BENCHEA, A.C., ZELINSCHI, C.B., DOROHOI, D.O., Rev. Chim. (Bucharest), **68**, no. 2, 2017, p. 307

Mauscript received: 18.12.2017